

1 **I. Title**

2 *Full title*

3 The Primary Tumor Immune Microenvironment Status Predicts the Response to Immunotherapy
4 and Overall Survival in Breast Cancer

5

6 *Short title*

7 Breast Cancer Primary Immune Microenvironment Predicts Immunotherapy Response and
8 Overall Survival

9

10 **Authors**

11 Arjun Moorthy, Imaging Endpoints, LLC Scottsdale, AZ; BASIS Scottsdale, Scottsdale, AZ

12 Aidan Quinn, Department of Pathology and Cell Biology, Columbia University, New York, NY;

13 Institute for Cancer Genetics, Columbia University Medical Center, New York, NY

14

15

16

17 **II. Abstract**

18 The tumor immune microenvironment (TIME) of breast cancer is a known source of tumor
19 heterogeneity and it has been increasingly recognized as having a role in the course of disease.
20 In the present study, we used a computational approach to dissect the landscape of TIME states
21 among TCGA breast cancer patients. Our central hypothesis is that the pre-existing TIME states
22 represent a dimension which is informative about the prognosis and the response to
23 immunotherapy. In order to test this hypothesis, we first classified breast cancer patients
24 according to their primary TIME status. Next, we describe a TIME-based classification with
25 prognostic value for overall survival among the TCGA patients. We further demonstrated that
26 absolute quantification of mast cells, M0 macrophages, CD8 T cells and neutrophils were
27 predictive of overall survival. In order to identify the TIME states which, predict response to
28 immune checkpoint blockade, we performed a similar analysis of 11 different mouse models of
29 primary invasive breast carcinoma that were subsequently treated with immune checkpoint
30 inhibitor (ICI) therapy. These analyses revealed that the TIME content of M1 macrophages,
31 monocytes and resting dendritic cells were predictive of sensitivity to ICI therapy. Taken together,
32 these results indicate that (1) the landscape of human primary TIME states is diverse and can
33 identify patients with more or less aggressive disease and (2) that pre-existing TIME states may
34 be able to identify patients, of all molecular subtypes of breast cancer, who are good candidates
35 for ICI therapy.

36

37

38 **III. Introduction**

39 Breast invasive adenocarcinoma is the most frequently diagnosed malignancy among
40 women in the United States, in 2020 it is expected to account for 15.3% of all new cancer
41 diagnoses and 42,170 of all cancer deaths.[1] Due largely to the development of aggressive and
42 improved treatment strategies as well as several targeted therapeutic agents, over the past two
43 decades the death rate of breast cancer has declined from about 31% in 1992 to 20% in 2017
44 with a 5 year survival rate of 90% between 2010-2016.[1] Despite these recent advances,
45 resistance to all known therapeutics still occurs in some women, especially those with basal
46 subtype tumors defined as HER2, PR and ER negative (or triple negative breast cancer), and
47 these patients inexorably progress in their disease.[2]

48 Notably, however, immunotherapies such as immune checkpoint inhibition (ICI) in
49 particular, have shown enormous potential in treating otherwise incurable carcinomas including
50 metastatic melanoma and lung cancer.[3,4] Recently, ICI treatments have proven to extend
51 survival among TNBC patients with metastatic disease. The IMpassion130 trial[5], demonstrated
52 that the anti-PDL1 therapy, atezolizumab in combination with nab-paclitaxel extended overall
53 survival compared to nab-paclitaxel alone among patients with tumors that express PDL-1.
54 However, the response rate among even patients with expression of PDL-1 was variable and
55 expression of PDL-1 alone is unlikely to fully account for the full spectrum of responses to
56 atezolizumab. Moreover, the IMpassion130 trial demonstrated that patients with metastatic
57 disease limited to lymph nodes received a far greater benefit from the atezolizumab, nab-
58 paclitaxel combination compared to those with distant metastases indicating a potential role for
59 ICI therapy at earlier stages in the disease. Taken together, these observations suggest that
60 breast cancer patient selection for ICI intervention is of critical importance and should be studied
61 in detail.

62 ICI therapies block the inactivation of the anti-tumor immune response by the tumor itself,
63 thus promoting immune-mediated cell killing of the tumor. Therefore, the primary tumor immune
64 microenvironment (TIME) may have a role in determining the effect of ICI therapies in breast
65 cancer by establishing a permissive or suppressive microenvironment for the immune system
66 thereby adding to or detracting from the effect of ICI therapy, respectively.

67 Recent efforts to identify biomarkers for and mechanisms of resistance to ICI therapy have
68 focused primarily on genetic or tumor intrinsic modes including the mutational burden of the
69 tumor[6] and the expression of ICI target molecules and immune modulating genes including PDL-
70 1 itself [7–9]. Relatively little, however, is known about the exact cellular composition of the
71 primary TIME of breast cancer in general and which TIME states specifically are predictive of ICI
72 response. Early work in identifying the TIME determinants of response to ICI therapy has
73 demonstrated the importance of the tumor lymphocyte (TIL) and macrophage abundance [10–12]
74 However, with recent the development of single cell high-throughput sequencing, studies have
75 begun to dissect the breast cancer TIME at the cell type compositional level [13,14]. Despite this
76 technological advancement, high cost and computational constraints remain and it is largely
77 infeasible to perform these experiments at the scale required to achieve the statistical power to
78 characterize the complete landscape of TIME statuses present among large, heterogenous
79 cohorts of breast cancer patients and associate trends in this landscape with clinical outcomes.

80 In the present study, we apply CIBERSORT [15], a computational approach to infer the
81 abundance of specific cell types from bulk RNA-seq data, to 922 individual samples of human
82 primary breast cancer from TCGA [16]. Using this approach, we were able to interrogate the
83 trends in the TIME statuses of these patients that are associated with prognosis of the disease.
84 In addition, we were able to apply a similar approach to mouse models of metastatic breast cancer
85 to identify TIME states that are predictive of objective response to ICI therapy in these models.

86

87

88 **IV. Materials and Methods**

89

90 **Human Primary Tumor RNA-seq Data**

91 Raw RNA-seq data and associated clinical metadata for 1,035 female patients with primary
92 breast invasive carcinoma in the TCGA database was downloaded using the GDC Data Portal.
93 Molecular subtype (Her2, Basal, or Luminal) was determined for each case using estrogen
94 receptor, progesterone receptor and HER2 status. Cases with equivocal or absent histological
95 measurements were excluded from further analysis (n = 113). Gene level summarized RNA-seq
96 read counts were normalized and statistical analyses performed using the R package DESeq2
97 [17].

98

99 **Mouse Primary Tumor RNA-seq Data**

100 Pre-treatment RNA-seq data from 47 individual animals comprising 11 different mouse models
101 of triple negative breast cancer was obtained from GEO (GSE124821). Briefly, and as detailed
102 by Hollern *et al.* in the original work [18], these animals were subsequently treated with anti-
103 CTLA4 and anti-PDL1 antibodies (bi-weekly, intraperitoneal injection) and objective response to
104 this combination therapy was recorded.

105

106 **Inference of Tumor Microenvironment Content from Bulk RNA-seq**

107 Scaled and normalized RNA-seq reads were imported into CIBERSORT [15] and TIME cell
108 content was inferred for all populations in the LM22 gene signature database. Immune cell
109 quantitation was performed with default parameters across 500 permutations run in relative and
110 absolute modes. Absolute quantification files were imported into R for downstream statistical
111 analysis and plotting.

112

113

114 **Statistical Analysis**

115 Survival analysis was performed in R using the survival package and Kaplan-Meier plots were
116 generated using the survminer package. All statistical tests were computed using base R v4.0.1.

117

118

119 **V. Results**

120

121 **TIME Landscape of Human Primary Invasive Breast Carcinoma**

122 In depth analysis and characterization of the TIME landscape of 1,035 primary samples
123 of human breast invasive carcinoma revealed profound variability in the constituent immune cell
124 types among patients (Figure 1a). Notably, high levels of all broadly detectable immune cell types
125 (macrophages, monocytes, resting mast cells, CD4 and CD8 T cells, B cells) were detected in
126 approximately 25% of all primary tumors - a feature indicative of immunologically hot tumors,
127 while 12% had low to undetectable levels (> 2 s.d. below the population mean) - indicative of
128 immunologically cold tumors. M2 macrophages and CD4 T resting memory cells were the most
129 frequently detected immune cell component of the breast cancer immune microenvironment,
130 detected in 98% and 92% of primary tumors, respectively. As expected, rare immunological cell
131 types such as neutrophils, eosinophils, activated mast cells, naive CD4 T cells, memory B cells
132 and $\gamma\delta$ T cells were only detected above background in 0-3% of primary tumors. Taken together,
133 these results indicate that CIBERSORT deconvolution of the TIME of human invasive breast
134 carcinoma recapitulates the expected variation among individuals and distribution of specific cell
135 types.

136

137 **Figure 1. Primary TIME States Segregate Human Invasive Breast Carcinoma into TIME**
138 **Classes with Functionally and Prognostically Distinct Features.** A. Heatmap of the primary
139 TIME landscape of human metastatic breast carcinoma. All 22 identifiable cell types are displayed

140 on the vertical axis and individual patients are clustered along the horizontal axis. Column colors
141 indicated the molecular subtype and the annotated front-line treatment type for each patient. B.
142 Kaplan-Meier plots for individual TIME cell types most predictive of overall survival. C.
143 Distributions of the absolute qualification of the key populations of TIME cells across the three
144 TIME classes. D. Kaplan-Meier plot comparing the overall survival among patients in the three
145 TIME classes. E. Cox-PH regression model testing the prognostic value of TIME classification
146 and molecular subtype. TIME-classification was predictive of overall survival independently of
147 molecular subtype. F. Gene set enrichment analysis comparing the transcriptional profiles of
148 aggressive TIME-classes 2 and 3 to class 1.

149

150 **TIME Features are Predictive of Prognosis in Primary Human Breast Tumors**

151 Given that the presence and/or absence of immune cells in the TIME have been shown to
152 influence the course of disease including invasiveness, metastasis and prognosis [19,20], we next
153 determined the relationship between overall survival and the TIME content of each individual cell
154 type within the LM22 signature set. The presence of high levels (> 25th percentile) of specific
155 lymphocyte types, Naive B cells ($p=0.0033$) and CD8 T cells ($p=0.0013$), conferred a significantly
156 better prognosis compared to patients with lower TIME content of these cells (Figure 1b).
157 Interestingly, patients with any detectable TIME content of neutrophils ($p=0.0056$) and eosinophils
158 ($p=0.0056$) had significantly worse prognosis compared to those without.

159 Based on the predictive capacity of lymphocytes and granulocytes in the primary breast
160 TIME, we designed a stronger classifier by aggregating the individual cell content information for
161 each of these individual cell types - which function as weak classifiers in our model. Patients with
162 naïve B cell content and CD8 T cell content higher than the 25th percentile for all patients and
163 undetectable neutrophil or eosinophil content were assigned to class 1 ($n = 131$). Patients with
164 the inverse TIME profiles were assigned to class 3 ($n = 144$), and patients that failed to fit into
165 either of these two groups were assigned to an intermediate class 2 ($n = 647$).

166 As expected, average CD8 T Cell and naïve B cell content were significantly higher in
167 class 1 patients compared to class 3 ($p < 2.2e-16$, Figure 1c). Class 2 patients tended to have
168 greater numbers of CD8 T cells and naïve B cells compared to those in class 3 ($p < 2.2e-16$), but
169 significantly lower than those in class 1 ($p < 2.2e-16$). Neutrophil and Eosinophil content was low
170 in both class 1 and class 2 patients but only significantly higher in class 3 compared to both
171 classes 1 and 2 ($p = 8.08e-10$ and $p = 0.0011$, respectively).

172 Consistent with the hypothesis that primary TIME status of primary tumors is predictive of
173 outcomes, our primary TIME classification strategy was able to identify patients significantly
174 different overall survival ($p < 0.0001$, Figure 1d). Moreover, this predictive capacity of the primary
175 TIME status remained statistically significant after controlling for molecular subtype (Figure 1e).
176 Patients with class 1 primary tumors had the best prognosis with a median overall survival of 11
177 years and greater than 90% survival rate beyond 9.6 years. Patients with class 2 tumors had an
178 intermediate prognosis with a median survival of 9.51 years and patients with class 3 tumors had
179 the worst prognosis with a median overall survival of only 5.83 years and fewer than 15%
180 achieving long-term survival beyond 8 years. After controlling for molecular subtype, patients with
181 class 2 tumors had hazard ratio of 3.5 (95% CI: 1.3 - 9.7, $p = 0.015$), compared to those with class
182 1 tumors, and patients with class 3 tumors had a hazard ratio of 11.2 (95% CI: 3.8 - 33.0, $p <$
183 0.001).

184

185 **Primary TIME Status is Predictive of Response to ICI Therapy**

186 Given the capacity of the human primary TIME to predict prognosis in the context of
187 conventional therapeutic strategies, we next sought to test whether the primary TIME was
188 informative for the response to immune checkpoint inhibition (ICI) therapy (Figure 2a).
189 CIBERSORT analysis was performed on publicly available RNA-seq data obtained from a panel
190 of 11 different mouse models of triple negative breast cancer, which were subsequently treated
191 with a combination of anti-PDL1 and anti-CTLA4 ICI and an objective response was measured.

192 This analysis revealed a heterogeneous primary TIME, qualitatively similar to that of the human
193 breast cancer tumors obtained from TCGA (Figure 2b).

194

195 **Figure 2. Primary TIME Status Predicts Response to Immune Checkpoint Inhibition**

196 **Therapy in Mouse Models of Breast Cancer.** A. Schematic of the experimental approach used

197 by Hollern *et al.* to generate the database of murine models of breast cancer response to ICI

198 treatment. B. Primary TIME landscape of the mouse models of invasive breast cancer; cell types

199 are displayed on the vertical axis and individual mice are clustered along the horizontal axis.

200 Column colors indicated the response to ICI treatment type for each animal. C. Percent of total

201 mice with primary TIME class (class 1, 2 or 3) separated by response to ICI therapy. D.

202 Distribution of the absolute quantification of the TIME cells most predictive of response among

203 ICI sensitive and resistant mice. E. Distribution of the ICI Response Scores of individual mice

204 separated by ICI response. F. ICI Response score for all 922 primary human tumor samples

205 included in the TCGA analysis separated by TIME class (class 1, 2 and 3).

206

207 Notable similarities to the human data include; high TIME content of M0 macrophages

208 was identified among approximately 65% of mouse tumors, M2 macrophage content was

209 consistently high in all tumors, high TIME content of plasma cells were identified in a minority of

210 tumors (<10%), and tumors were largely devoid of rare immune cell populations such as

211 neutrophils.

212 We next determined the TIME class of the mouse models according to our method

213 described above. The distribution of TIME classifications of these mouse models closely

214 resembled the distribution of time classifications among the human tumors, with class 1 tumors

215 comprising 14.9%, class 2 comprising 59.5% and class 3 comprising 25.5% of mouse tumors. As

216 expected, the TIME class of the ICI-sensitive mice was lower on average compared to those that

217 were resistant to ICI therapy (figure 2c).

218 Consistent with other reports, our analysis revealed that TIME content of lymphocytes was
219 predictive of the objective response to ICI treatment (supplemental figure 1). Specifically, plasma
220 cell, CD8 T cell and CD4 memory T cell contents were significantly associated with response.

221

222 **TIME Based ICI Response Score**

223 In order to more quantitatively and sensitively identify TIME statuses which could be
224 predictive of ICI therapy response, we next compared the predictive capacity of each individual
225 TIME components and developed an ICI Response Score (RS) on the basis of the top individual
226 predictors - M1 macrophages, monocytes and resting dendritic cells (figure 2d).

227 Briefly, the CIBERSORT absolute quantifications for each sample i , were used to
228 compute the quantity

229

$$230 \quad RS_i = \max\{|DC_i^R|, (|M_i^0| + |Mc_i|)\},$$

231

232 where DC^R is the resting dendritic cell content, M^0 is the M0 macrophage content and Mc is the
233 monocyte content.

234 The ICI Response Score of the primary TIME was significantly higher among animals that
235 objectively responded (mean RS of 25, +/- 13 *s.d.*) compared to those that did not respond (mean
236 $RS = 75$, +/- 20 *s.d.*, $p = 2.1 \times 10^{-6}$), indicating that this response score may be useful to identify
237 breast cancer patients who could benefit from ICI therapy.

238 Next, to determine whether RS was associated with a particular TIME class in human
239 patients, we computed the RS for each patient in our TCGA data set (figure 2f). This analysis
240 revealed that patients with class 3 primary TIME status had significantly lower RS, compared to
241 those in class 1 ($p < 0.001$). However, we were able to identify patients of all primary TIME classes
242 and molecular subtypes with high RS's indicating that this subset of breast cancer patients might
243 respond well to ICI therapy.

244

245 **VI. Discussion**

246 The role of the tumor immune microenvironment in the course of disease of breast cancer
247 including prognosis and response to cancer immunotherapies remains poorly understood. In this
248 study we used an unbiased computational approach to infer the cellular composition of the
249 primary TIME of 922 patients from bulk RNA-seq data. From this rich dataset we were able to
250 identify primary TIME states that are informative for prognosis indecently of molecular subtype in
251 human breast cancer. In addition, we identified pre-existing TIME states that are related to
252 response to immune checkpoint inhibition in a panel of mouse models of invasive breast
253 carcinoma, indicating the utility of this approach to dissecting the primary TIME for predicting
254 response to ICI therapy.

255 Previous studies aimed at elucidating the primary breast cancer TIME have generally
256 either examined a small subset of TIME components among a large cohort of patients or taken a
257 less biased approach such as single cell RNA-seq to carefully dissect the TIME status of smaller
258 numbers patients [21]. Here, using computational methods to infer the absolute quantifications of
259 22 different immune cell populations from the bulk RNA-sequencing data we were able to perform
260 a less biased study of a large cohort of patients. This approach allowed us to identify a highly
261 variable landscape of primary TIME states among the TCGA breast cancer patients. Suggesting
262 that there is a high degree of inter-tumoral variability in the TIME content, which has been
263 postulated to underly differential responses to both traditional and immunotherapies [22].

264 Specifically, the relationship between tumor lymphocyte content and overall survival are
265 supported by our data, however we additionally identify that high neutrophil and eosinophil content
266 confers a worse overall prognosis. Our novel primary TIME-based classification strategy
267 incorporates these findings and demonstrates that the TIME state of the primary tumor indeed
268 has prognostic value, independently of the molecular subtype of the tumor.

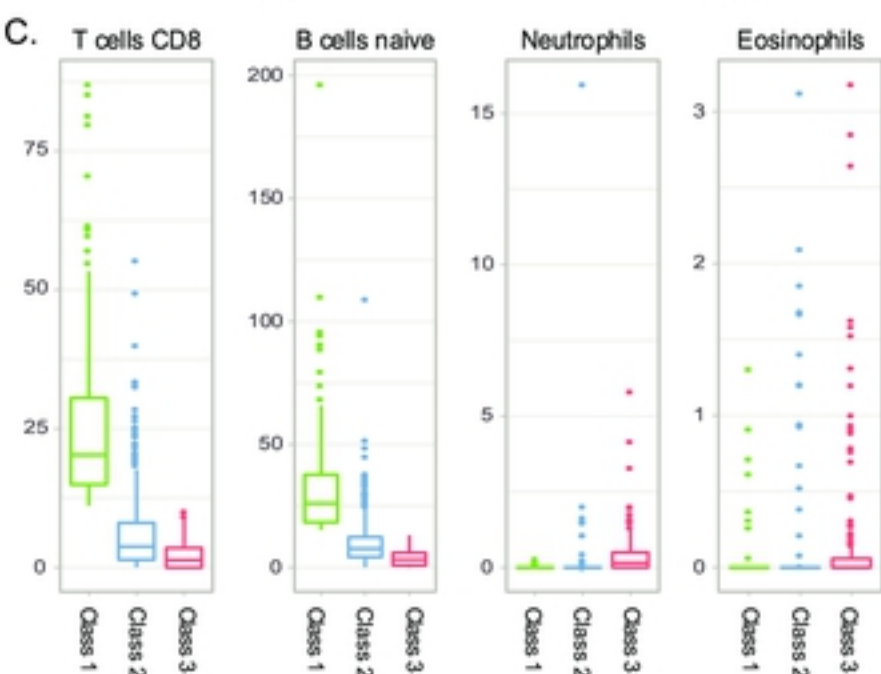
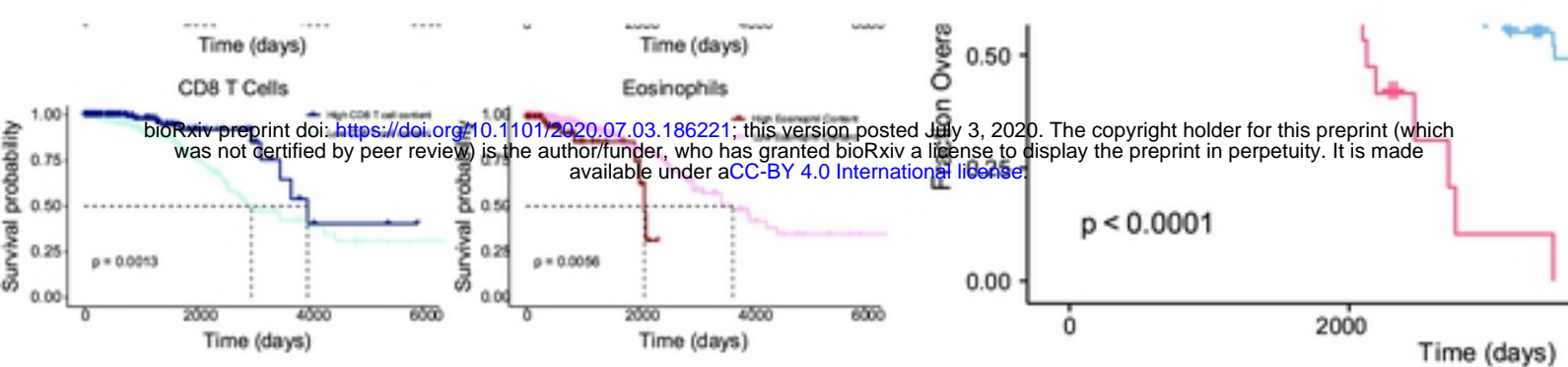
269 Furthermore, in order to use the primary TIME status to identify those patients who could
270 benefit from immune checkpoint inhibition therapy, we developed an ICI Response Score based
271 on primary TIME status. A subset of patients of all molecular subtypes and primary TIME classes
272 were identified with high ICI Response Scores, suggesting that future ICI therapy preclinical and
273 clinical trials would benefit from stratification methods which consider the primary TIME prior to
274 enrolment.

275 Taken together, these findings demonstrate that pre-existing TIME states are relevant to
276 both the prognosis of breast cancer patients and to the choice of therapy. Future studies should
277 further dissect these TIME states by flow cytometric and/or single cell RNA-sequencing
278 approaches in prospective studies.

- 279 1. Surveillance, Epidemiology, and End Results Program (SEER). 1 May 2020. Available:
280 <https://seer.cancer.gov>
- 281 2. Nedeljković M, Damjanović A. Mechanisms of Chemotherapy Resistance in Triple-Negative
282 Breast Cancer—How We Can Rise to the Challenge. *Cells*. 2019;8: 957.
283 doi:10.3390/cells8090957
- 284 3. Darvin P, Toor SM, Sasidharan Nair V, Elkord E. Immune checkpoint inhibitors: recent
285 progress and potential biomarkers. *Exp Mol Med*. 2018;50: 1–11. doi:10.1038/s12276-018-
286 0191-1
- 287 4. Havel JJ, Chowell D, Chan TA. The evolving landscape of biomarkers for checkpoint inhibitor
288 immunotherapy. *Nat Rev Cancer*. 2019;19: 133–150. doi:10.1038/s41568-019-0116-x
- 289 5. Schmid P, Adams S, Rugo HS, Schneeweiss A, Barrios CH, Iwata H, et al. Atezolizumab and
290 Nab-Paclitaxel in Advanced Triple-Negative Breast Cancer. *N Engl J Med*. 2018;379:
291 2108–2121. doi:10.1056/NEJMoa1809615
- 292 6. Schrock AB, Ouyang C, Sandhu J, Sokol E, Jin D, Ross JS, et al. Tumor mutational burden is
293 predictive of response to immune checkpoint inhibitors in MSI-high metastatic colorectal
294 cancer. *Ann Oncol*. 2019;30: 1096–1103. doi:10.1093/annonc/mdz134
- 295 7. Taube JM, Young GD, McMiller TL, Chen S, Salas JT, Pritchard TS, et al. Differential
296 Expression of Immune-Regulatory Genes Associated with PD-L1 Display in Melanoma:
297 Implications for PD-1 Pathway Blockade. *Clin Cancer Res*. 2015;21: 3969–3976.
298 doi:10.1158/1078-0432.CCR-15-0244
- 299 8. Seidel JA, Otsuka A, Kabashima K. Anti-PD-1 and Anti-CTLA-4 Therapies in Cancer:
300 Mechanisms of Action, Efficacy, and Limitations. *Front Oncol*. 2018;8: 86.
301 doi:10.3389/fonc.2018.00086
- 302 9. Davis AA, Patel VG. The role of PD-L1 expression as a predictive biomarker: an analysis of
303 all US Food and Drug Administration (FDA) approvals of immune checkpoint inhibitors. *J*
304 *Immunother Cancer*. 2019;7: 278. doi:10.1186/s40425-019-0768-9
- 305 10. Chen P-L, Roh W, Reuben A, Cooper ZA, Spencer CN, Prieto PA, et al. Analysis of
306 Immune Signatures in Longitudinal Tumor Samples Yields Insight into Biomarkers of
307 Response and Mechanisms of Resistance to Immune Checkpoint Blockade. *Cancer*
308 *Discov*. 2016;6: 827–837. doi:10.1158/2159-8290.CD-15-1545
- 309 11. Beyrend G, van der Gracht E, Yilmaz A, van Duikeren S, Camps M, Höllt T, et al. PD-L1
310 blockade engages tumor-infiltrating lymphocytes to co-express targetable activating and
311 inhibitory receptors. *J Immunother Cancer*. 2019;7: 217. doi:10.1186/s40425-019-0700-3
- 312 12. McGranahan N, Furness AJS, Rosenthal R, Ramskov S, Lyngaa R, Saini SK, et al. Clonal
313 neoantigens elicit T cell immunoreactivity and sensitivity to immune checkpoint blockade. :
314 8.
- 315 13. Chung W, Eum HH, Lee H-O, Lee K-M, Lee H-B, Kim K-T, et al. Single-cell RNA-seq
316 enables comprehensive tumour and immune cell profiling in primary breast cancer. *Nat*
317 *Commun*. 2017;8: 15081. doi:10.1038/ncomms15081

- 318 14. Kim C, Gao R, Sei E, Brandt R, Hartman J, Hatschek T, et al. Chemoresistance Evolution
319 in Triple-Negative Breast Cancer Delineated by Single-Cell Sequencing. *Cell*. 2018;173:
320 879-893.e13. doi:10.1016/j.cell.2018.03.041
- 321 15. Newman AM, Liu CL, Green MR, Gentles AJ, Feng W, Xu Y, et al. Robust enumeration of
322 cell subsets from tissue expression profiles. *Nat Methods*. 2015;12: 453–457.
323 doi:10.1038/nmeth.3337
- 324 16. The Cancer Genome Atlas Program. 1 May 2020. Available: <https://www.cancer.gov/tcga>
- 325 17. Love MI, Huber W, Anders S. Moderated estimation of fold change and dispersion for
326 RNA-seq data with DESeq2. *Genome Biol*. 2014;15: 550. doi:10.1186/s13059-014-0550-8
- 327 18. Hollern DP, Xu N, Thennavan A, Glodowski C, Garcia-Recio S, Mott KR, et al. B Cells and
328 T Follicular Helper Cells Mediate Response to Checkpoint Inhibitors in High Mutation
329 Burden Mouse Models of Breast Cancer. *Cell*. 2019;179: 1191-1206.e21.
330 doi:10.1016/j.cell.2019.10.028
- 331 19. Tower, Ruppert, Britt. The Immune Microenvironment of Breast Cancer Progression.
332 *Cancers*. 2019;11: 1375. doi:10.3390/cancers11091375
- 333 20. Baxevasis CN, Sofopoulos M, Fortis SP, Perez SA. The role of immune infiltrates as
334 prognostic biomarkers in patients with breast cancer. *Cancer Immunol Immunother*.
335 2019;68: 1671–1680. doi:10.1007/s00262-019-02327-7
- 336 21. Fridman WH, Pagès F, Sautès-Fridman C, Galon J. The immune contexture in human
337 tumours: impact on clinical outcome. *Nat Rev Cancer*. 2012;12: 298–306.
338 doi:10.1038/nrc3245
- 339 22. Divya Nagarajan, Stephanie McArdle. Immune Landscape of Breast Cancers.
340 *Biomedicines*. 2018;6: 20. doi:10.3390/biomedicines6010020

341



E.

TIME Classification	Class 1 (n=131)	reference
Class 2 (n=647)	3.5 (1.3 - 9.7)	
Class 3 (n=144)	11.2 (3.8 - 33.0)	
Molecular Subtype	Luminal (n=659)	reference
Her2 (n=158)	2.7 (1.6 - 4.7)	
Basal (n=105)	2.0 (1.0 - 3.9)	

N events: 82; Global p-value (Log-Rank): 2.7154e-08
AIC: 784.68; Concordance Index: 0.7

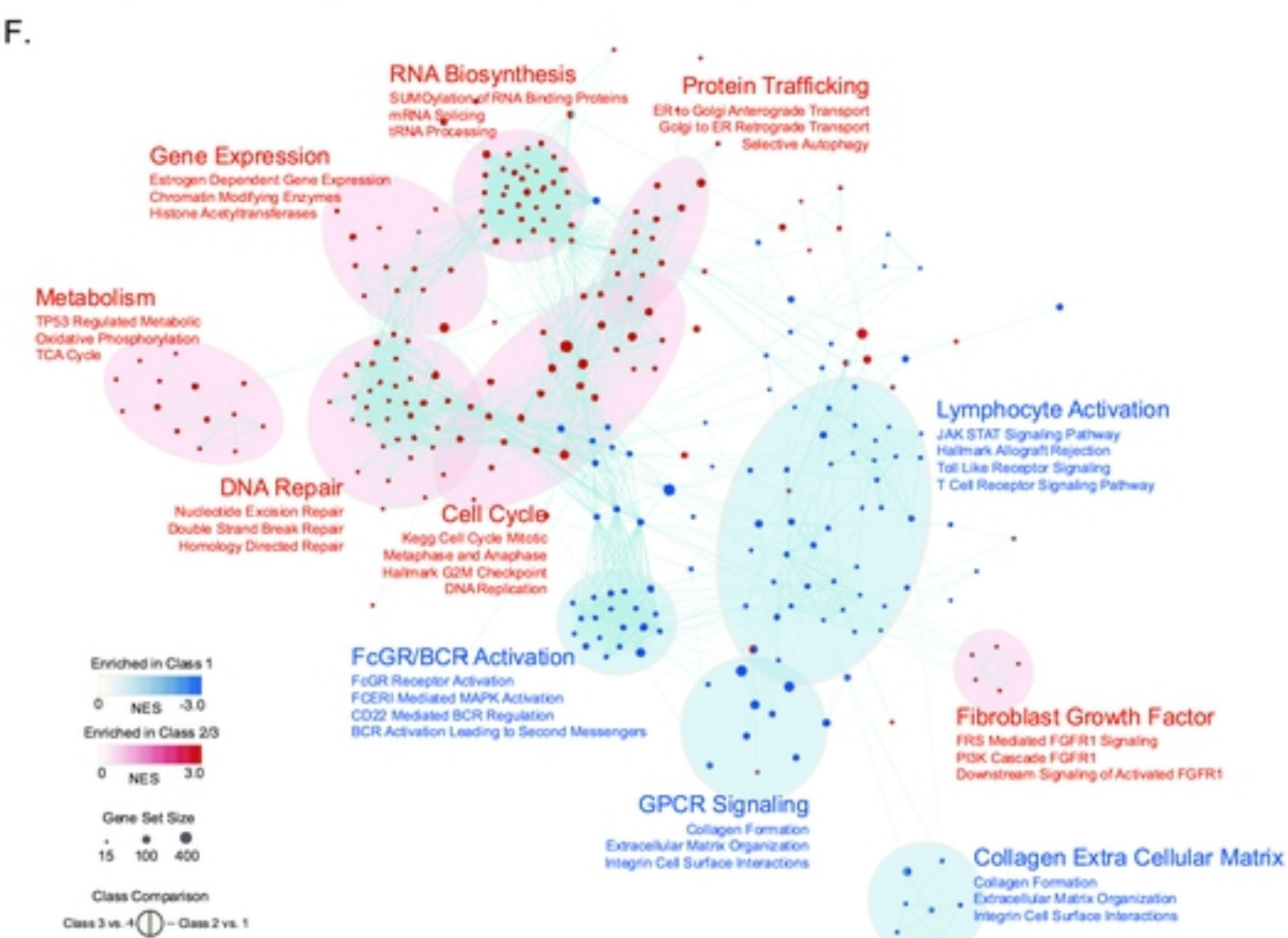
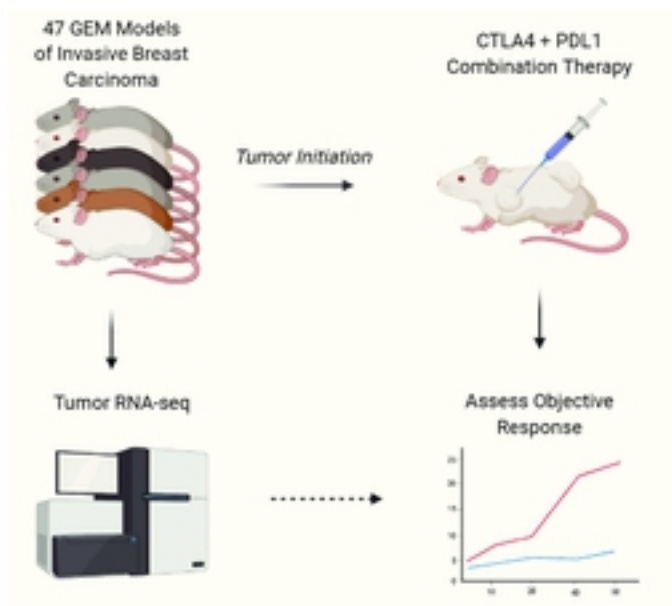


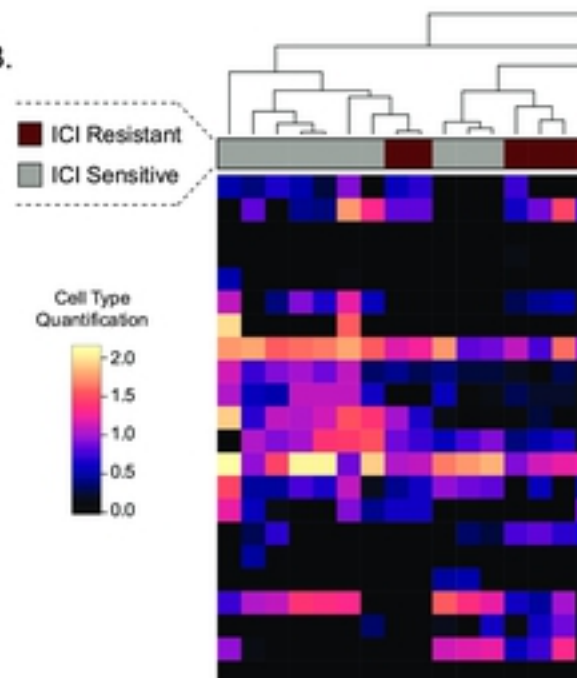
Figure 1

Figure 2

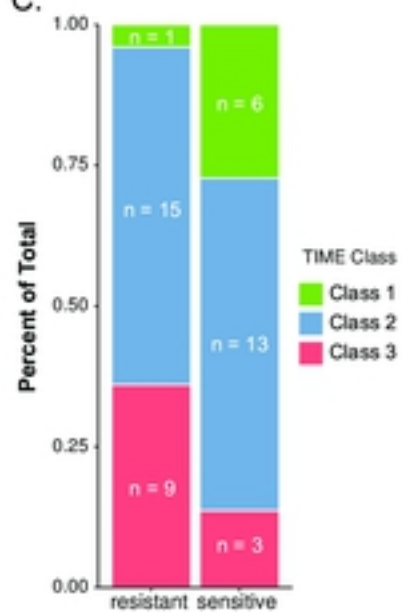
A.



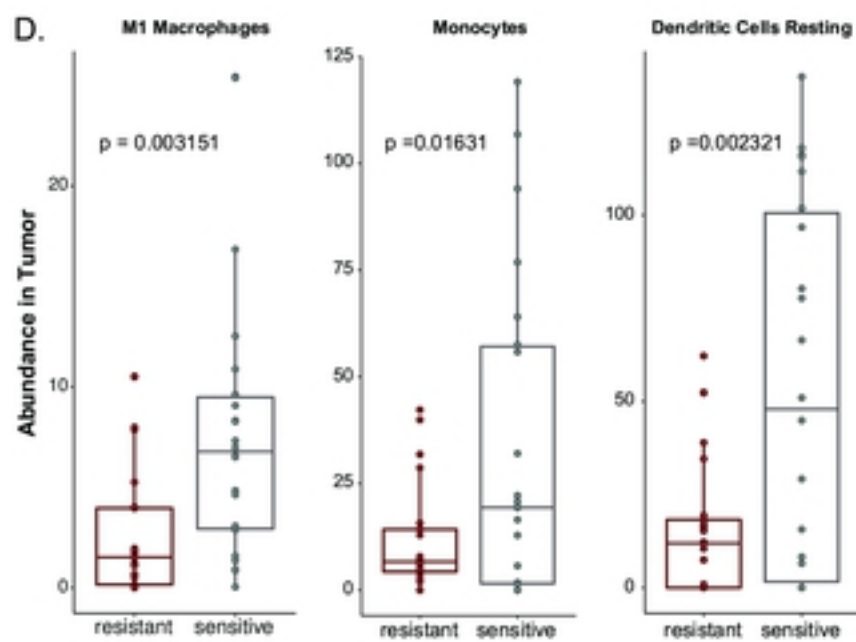
B.



C.



D.



E.



Figure 2